



Performance Analysis in Double-Rayleigh Channels with Diversity Combining Techniques

Mohamed Lassaad Ammari¹ · Sébastien Roy²

Published online: 27 May 2020
© Springer Science+Business Media, LLC, part of Springer Nature 2020

Abstract

In this paper, we provide a performance analysis of communication systems over Rayleigh-product channels with two popular diversity combining techniques, namely maximal ratio combining (MRC) and selection combining (SC). We first derive new closed-form expressions for the exact cumulative distribution function (CDF) and probability density function (PDF) of the post-processing signal-to-noise ratio (SNR) for these two schemes. Secondly, we present the first-order asymptotic expansions for these CDF and PDF functions. Performance of MRC and SC techniques, in terms of outage probability, average symbol error rate (SER) and ergodic capacity, is derived using the exact expressions of CDF and PDF. Furthermore, we present new expressions for key metrics characterizing the system performance at the high and low SNR regimes. Thanks to the asymptotic CDF and PDF expressions, we compute the average SER in the high SNR regime and derive the diversity order and array gain parameters. In addition, we provide simple expressions for the ergodic capacity in the asymptotic low and high SNR regimes. Monte-Carlo simulations are conducted and their results agree well with the analytical results.

Keywords MIMO systems · Performance analysis · Rayleigh-product channels

1 Introduction

Spatial diversity, which combines multiple replicas of the received signal, has long been recognized as an effective technique to mitigate fading and its impact on the performance of communication systems [1, 2]. Receiver diversity combining methods such as maximal ratio combining (MRC), equal gain combining (EGC) and selection combining (SC) are often used to combine available diversity branches [1–3]. It is well known that, in the ideal case of independent diversity branches, MRC is the optimal technique in terms of maximizing

✉ Mohamed Lassaad Ammari
mlammari@gel.ulaval.ca

Sébastien Roy
sebastien.roy13@usherbrooke.ca

¹ NOCCS Laboratory, National Engineering School of Sousse, University of Sousse, 4002 Sousse, Tunisia

² Department of Electrical and Computer Engineering, University of Sherbrooke, Québec, Canada

the SNR at the combiner output [1–3]. However, for MRC, the multiple radio frequency (RF) chains associated with each branch increase the cost and the signal processing complexity of the receiver. On the other hand, SC is one of the simplest suboptimal combining scheme, in which the receiver selects the diversity branch having the highest instantaneous SNR [1–3]. The performance of MRC and SC techniques has been extensively investigated under various fading channels, including Rayleigh, Nakagami- m , and Rician (see references in [4–6]). Previous works have shown that the diversity gain depends on the statistical correlation among the fading envelopes of the signals received at the different branches [7–9]. Hence, the maximum diversity gain is obtained when the fading processes at the branches are independent. The impact of spatial correlation on the performance of MRC and SC techniques is well studied (see e.g., [8–12]). Furthermore, prior works are based on the assumption of a perfect scattering environment. Under this hypothesis, the covariance matrix of the channel vector has full-rank.

Recently, field measurements have shown that the lack of scatterers around the transmitter and the receiver may reduce the channel matrix rank [13, 14]. To characterize this phenomenon, a new channel model for multiple-input multiple-output (MIMO) systems has been proposed in [13]. This double-scattering model takes into account both rank-deficiency and spatial correlation by modeling the MIMO channel as a product of two statistically independent complex Gaussian matrices and three deterministic matrices. The latter correspond to the transmitter, receiver, and scatterer correlation matrices. The double Rayleigh (or Rayleigh-product) model is a special case of the double-scattering model, where all three correlation matrices are equal to the identity matrix [15]. In contrast to rich-scattering, analytical performance assessment under double-scattering channels are relatively rare. In [16], authors have presented a performance analysis of transmit beamforming (BF) systems in Rayleigh product channels. To characterize the statistical properties of the received signal-to-noise ratio (SNR), Jin et al. have derived new closed-form expressions for the cumulative distribution function (CDF), probability density function (PDF), and moments of the maximum eigenvalue of a product of independent complex Gaussian matrices. The performance of an interference-limited double scattering MIMO channel with optimum combining is presented in [17]. For mathematical simplicity, authors have assumed that the number of co-channel interferers is greater than or equal to the number of receive antennas and the impact of noise was neglected. This assumption has been relaxed in [18] where authors have investigated the performance of a MIMO-BF system in Rayleigh-product channels with arbitrary-power co-channel interference. In [15], Rayleigh-product MIMO channels with linear receivers are considered and exact closed-form expressions for the ergodic sum-rate are derived. The performance of double-scattering channels with diversity combining techniques has been investigated in [19, 20]. In [19], double Nakagami- m channels with MRC diversity are considered, while authors in [20] have focused on double Rayleigh fading channels with EGC. The double-scattering propagation was modeled as a double-generalized Gamma (dGG) distribution in [21], where an analytical framework has been derived to analyze the performance of a transmit antenna selection system operating in vehicle-to-vehicle communication channels.

In this paper, we consider the performance of SC and MRC combining techniques in uncorrelated double-Rayleigh channels. First, we derive new closed-form expressions and asymptotic expansions for the PDF and the CDF of the SNR at each combiner output. Based on these expressions, we then investigate the performance of SC and MRC in terms of outage probability, average symbol error rate (SER), and ergodic capacity. In addition, in order to obtain the diversity order and array gain of the considered techniques, asymptotic SER expressions are derived. Furthermore, simple expressions for the ergodic capacity

in the asymptotic low and high SNR regimes are provided. The main contribution of this paper is the derivation of the closed-form expressions for the CDF and PDF of the SNR at both SC and MRC output. It is noted that the PDF of the SNR at the MRC combiner output in double Nakagami- m channels has been derived in [19]. In [19], the fading coefficient in each diversity branch is expressed as the product of two independent Nakagami- m fading coefficients. In contrast with [19] and as we will see, the fading in this paper is the sum of many products of two independent Rayleigh fading coefficients. Moreover, the MRC system considered in this paper differs from that studied in [16] where a MIMO-BF system is investigated. In fact, the SNR of the MIMO-BF approach depends explicitly on the maximum eigenvalue of the MIMO channel.

The notation adopted in this paper conforms to the following conventions. Scalars are denoted by lower case letters, vectors by bold lower case letters and matrices by bold upper case letters. The symbol \mathbf{I}_n denotes the identity matrix of size n . Superscript $(\cdot)^H$ denotes the Hermitian operation, the Frobenius norm of a matrix \mathbf{A} is denoted by $\|\mathbf{A}\|_F$ and $[\mathbf{A}]_{ij}$ refers to the (i, j) th element of a matrix \mathbf{A} .

The remainder of this manuscript is organized as follows. In Sect. 2, we introduce the system and the double-Rayleigh channel models. Section 3 provides the exact expressions and the asymptotic expansions of the CDF and PDF of the SNR. The performance of SC and MRC combiners are investigated in Sect. 4. Finally, a conclusion to this work is provided in Sect. 5.

2 System Model

Consider N_r -branch diversity reception over Rayleigh-product fading channels. Following [15–18], we assume that the channel vector $\mathbf{h} = [h_1, \dots, h_{N_r}]^T$ has the statistical factorization given by

$$\mathbf{h} = \frac{1}{\sqrt{N_s}} \mathbf{H}_1 \mathbf{g}, \quad (1)$$

where $\mathbf{H}_1 = [h_{1,ij}] \in \mathbb{C}^{N_r \times N_s}$ and $\mathbf{g} = [g_i] \in \mathbb{C}^{N_s \times 1}$ are mutually independent matrices with independent identically distributed (i.i.d.) entries that follow a zero-mean unit-variance complex-Gaussian distribution and N_s is the number of effective scatterers. Hereafter, we refer to this channel model by (N_r, N_s) . The generic model of (1) includes the extreme cases of the rich-scattering Rayleigh fading ($N_s \rightarrow \infty$) and the keyhole channel ($N_s = 1$) [16]. Let E_s and N_0 denote the average transmit energy per symbol and the one-sided power spectral density of the zero-mean additive white Gaussian, respectively.

In this paper, the MRC and SC combining schemes are considered. We assume that the fading channel is quasi-static, i.e. that fading coefficients remain invariant within one frame and change independently from one frame to another. It is also assumed that the channel state information (CSI) is perfectly available to the receiver.

For the MRC scheme, all the N_r receive antennas are combined to generate the output. The instantaneous received SNR after combining is then

$$\gamma_{\text{MRC}} = \bar{\gamma} \|\mathbf{h}\|_F^2, \quad (2)$$

where $\bar{\gamma} = E_s/N_0$. For the SC scheme, a single receive antenna, the one with the largest instantaneous SNR, is selected. Let α be the index of the selected antenna. The instantaneous received SNR at the SC output is

$$\gamma_{SC} = \bar{\gamma} |h_\alpha|^2. \tag{3}$$

In the remainder of this paper, we use the following notation

$$\gamma_i = \bar{\gamma} \beta_i, \quad \text{for } i \in \{\text{MRC, SC}\}, \tag{4}$$

where $\beta_{\text{MRC}} = \|\mathbf{h}\|_F^2$ and $\beta_{\text{SC}} = |h_\alpha|^2$.

3 Statistical Proprieties of the SNR

In this section, we first derive new expressions for the exact and asymptotic CDF and PDF of the SNR at the output of the MRC and SC combiners. These statistical functions will be used in the next section to evaluate system performance.

3.1 Exact Expressions for the CDF and the PDF

Proposition 1 *The CDF and PDF of γ_{MRC} are, respectively, given by*

$$F_{\gamma_{\text{MRC}}}(x) = 1 - \sum_{k=0}^{N_r-1} \frac{2K_{N_s-k}(2\sqrt{xN_s/\bar{\gamma}})}{\Gamma(N_s)k!} \left(\frac{xN_s}{\bar{\gamma}}\right)^{(N_s+k)/2}, \tag{5}$$

and

$$f_{\gamma_{\text{MRC}}}(x) = \frac{2x^{\frac{N_s+N_r}{2}-1} K_{N_s-N_r}(2\sqrt{xN_s/\bar{\gamma}})}{\Gamma(N_r)\Gamma(N_s)} \left(\frac{N_s}{\bar{\gamma}}\right)^{(N_s+N_r)/2}, \tag{6}$$

where $K_v(\cdot)$ is the v th order modified Bessel function of the second kind.

Proof See Appendix 6. □

Proposition 2 *The CDF and PDF of γ_{SC} are, respectively, given by*

$$F_{\gamma_{\text{SC}}}(x) = 1 + \sum_{k=1}^{N_r} \binom{N_r}{k} \frac{2(-1)^k}{\Gamma(N_s)} \left(\frac{kxN_s}{\bar{\gamma}}\right)^{N_s/2} K_{N_s}(2\sqrt{kxN_s/\bar{\gamma}}), \tag{7}$$

and

$$f_{\gamma_{\text{SC}}}(x) = \sum_{k=1}^{N_r} \binom{N_r}{k} \frac{2kN_s(-1)^{k+1}}{\Gamma(N_s)\bar{\gamma}} \left(\frac{kxN_s}{\bar{\gamma}}\right)^{(N_s-1)/2} K_{N_s-1}(2\sqrt{kxN_s/\bar{\gamma}}). \tag{8}$$

Proof See Appendix 7. □

Fig. 1 CDF $F_{\gamma_{\text{MRC}}}(\gamma)$ for different scenarios (N_r, N_s) and $\bar{\gamma} = 5$ dB

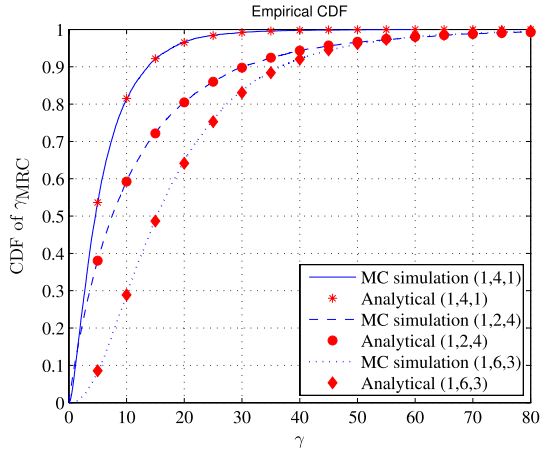
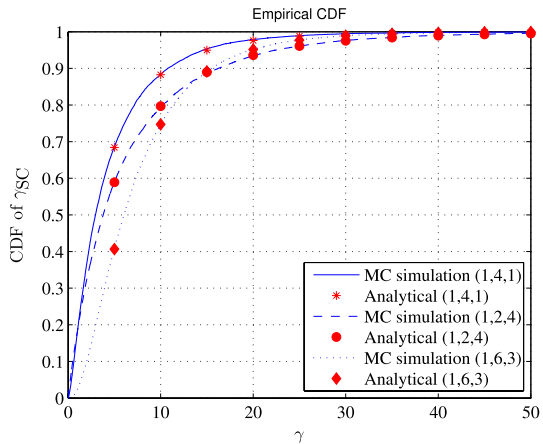


Fig. 2 CDF $F_{\gamma_{\text{SC}}}(\gamma)$ for different scenarios (N_r, N_s) and $\bar{\gamma} = 5$ dB



Figures 1 and 2 show the CDF of the SNR at the MRC and SC combiners for different channel models (N_r, N_s) and $\bar{\gamma} = 5$ dB. The analytical results are obtained by (5) and (7) and the simulated curves are generated by Monte-Carlo simulations carried out over 10^5 independent channel realizations. We can see an excellent agreement between the analytical and simulated results.

3.2 Asymptotic Expressions for the CDF and the PDF

Here, we consider the high SNR regime and derive the first-order expansions for the CDF and the PDF given in (5)–(8). These asymptotic expressions will constitute a basis from which to evaluate the diversity order and the array gain of the considered systems.

To obtain such asymptotic expressions, we use the series representation of $K_\nu(\cdot)$, given by [22, Eq. (8.446)], and express $K_\nu(2\sqrt{z})$ as

$$\begin{aligned}
 K_v(2\sqrt{z}) &= \underbrace{\frac{1}{2} \sum_{l=0}^{v-1} (-1)^l \frac{(v-l-1)!}{l!} z^{l-v/2}}_{\text{Term I}} \\
 &+ \underbrace{\frac{(-1)^{v+1}}{2} \sum_{l=0}^{\infty} \frac{1}{l!(v+l)!} z^{(l+v/2)} [\ln z - \Psi(v, l)]}_{\text{Term II}},
 \end{aligned}
 \tag{9}$$

where $\Psi(v, l) = \psi(l + 1) + \psi(v + l + 1)$ and $\psi(\cdot)$ is Euler’s digamma function.

3.2.1 Case I: MRC with $N_r \neq N_s$

Given the first order of the expansion in (9), we express the asymptotic PDF of γ_{MRC} as follows

$$f_{\gamma_{\text{MRC}}}^{\infty}(x) = \frac{\Gamma(|N_s - N_r|)}{\Gamma(N_r)\Gamma(N_s)} \left(\frac{N_s}{\bar{\gamma}}\right)^s x^{s-1} + o(x^{s-1}),
 \tag{10}$$

where $s = \min(N_s, N_r)$. Using Proposition I in [23], we approximate the CDF of γ_{MRC} in the high SNR regime as

$$F_{\gamma_{\text{MRC}}}^{\infty}(x) = \frac{\Gamma(|N_s - N_r|)}{s\Gamma(N_r)\Gamma(N_s)} \left(\frac{N_s}{\bar{\gamma}}\right)^s x^s + o(x^s).
 \tag{11}$$

3.2.2 Case II: MRC with $N_r = N_s$

Using (9), we express the PDF as

$$f_{\gamma_{\text{MRC}}}^{\infty}(x) = \frac{1}{[\Gamma(N_s)]^2} \left(\frac{N_s}{\bar{\gamma}}\right)^{N_s} x^{N_s-1} \ln\left(\frac{\bar{\gamma}}{xN_s}\right).
 \tag{12}$$

To derive the CDF, we use Proposition I in [23]. First, we note that $\ln(x)$ is a slowly¹ varying function at $+\infty$, since $\lim_{x \rightarrow \infty} \ln(tx)/\ln(x) = 1$. Then, by virtue of [23, Proposition I], we obtain

$$F_{\gamma_{\text{MRC}}}^{\infty}(x) = \frac{1}{N_s[\Gamma(N_s)]^2} \left(\frac{N_s}{\bar{\gamma}}\right)^{N_s} x^{N_s} \ln\left(\frac{\bar{\gamma}}{xN_s}\right).
 \tag{13}$$

3.2.3 Case III: SC Scheme with $N_s \leq N_r$

For the SC scheme, we can express the CDF as

¹ For the definition of slowly varying function, please see [23, 24].

$$\begin{aligned}
 F_{\gamma_{sc}}^\infty(x) = & \underbrace{1 + \sum_{k=1}^{N_r} \sum_{l=0}^{N_s} \binom{N_r}{k} \frac{(-1)^{k+l} (N_s - l - 1)!}{\Gamma(N_s) l!} \left(\frac{kxN_s}{\bar{\gamma}}\right)^l}_{\text{Term I}} \\
 & + \sum_{k=1}^{N_r} \binom{N_r}{k} \frac{(-1)^{N_s+k+1}}{\Gamma(N_s)} \sum_{l=0}^\infty \left\{ \frac{1}{l!(N_s + l)!} \right. \\
 & \left. \times \left(\frac{kxN_s}{\bar{\gamma}}\right)^{(N_s+l)} \left[\ln\left(\frac{kxN_s}{\bar{\gamma}}\right) - \Psi(N_s, l) \right] \right\}.
 \end{aligned} \tag{14}$$

Using [22, Eq. (0.154)], we have

$$\begin{aligned}
 \sum_{k=1}^{N_r} \binom{N_r}{k} (-1)^k &= -1, \\
 \sum_{k=1}^{N_r} \binom{N_r}{k} (-1)^l k &= 0, \text{ for } 1 \leq l \leq N_r - 1.
 \end{aligned} \tag{15}$$

Now, it is convenient to consider two cases $N_s \leq N_r$ and $N_s > N_r$.

For $N_s \leq N_r$, using (15), we can easily see that Term I in (14) equates to zero. The CDF in the high SNR regime can be obtained from the first-order term as

$$\begin{aligned}
 F_{\gamma_{sc}}^\infty(x) = & \sum_{k=1}^{N_r} \left\{ \binom{N_r}{k} \frac{(-1)^{k+N_s+1}}{\Gamma(N_s)\Gamma(N_s + 1)} \right. \\
 & \left. \times \left(\frac{kxN_s}{\bar{\gamma}}\right)^{N_s} \ln\left(\frac{kxN_s}{\bar{\gamma}}\right) \right\}.
 \end{aligned} \tag{16}$$

The asymptotic PDF is given by

$$\begin{aligned}
 f_{\gamma_{sc}}^\infty(x) = & \sum_{k=1}^{N_r} \left\{ \binom{N_r}{k} \frac{(-1)^{k+1+N_s}}{[\Gamma(N_s)]^2} \right. \\
 & \left. \times \left(\frac{kxN_s}{\bar{\gamma}}\right)^{N_s} x^{N_s-1} \ln\left(\frac{kxN_s}{\bar{\gamma}}\right) \right\}.
 \end{aligned} \tag{17}$$

3.2.4 Case IV: SC Scheme with $N_s > N_r$

For $N_s > N_r$, Term I in (14) is not equal to zero. We can see that the leading unity term in Term I is canceled by the summation from $l = 0$ to $l = N_r - 1$. Hence, the CDF expansion is dominated by Term I for $l = N_r$. The asymptotic CDF is then given by

$$F_{\gamma_{sc}}^\infty(x) = \sum_{k=1}^{N_r} \binom{N_r}{k} \frac{(-1)^{N_r+k} (N_s - N_r - 1)!}{\Gamma(N_s) N_r!} \left(\frac{kxN_s}{\bar{\gamma}}\right)^{N_r}. \tag{18}$$

The asymptotic PDF can be expressed as

$$f_{\gamma_{SC}}^\infty(x) = \sum_{k=1}^{N_r} \left\{ \binom{N_r}{k} (-1)^{k+N_r} \times \frac{kN_s(N_s - N_r - 1)!}{\Gamma(N_s)\bar{\gamma}(N_r - 1)!} \left(\frac{kxN_s}{\bar{\gamma}}\right)^{N_r-1} \right\}. \tag{19}$$

It is noted that for the four cases, the asymptotic CDF scales inversely to $s = \min(N_s, N_r)$.

3.3 Generalized SNR Moments

The t th moment of the SNR at the MRC output is

$$\mathbb{E}\{\gamma_{MRC}^t\} = \frac{\Gamma(N_s + t)\Gamma(N_r + t)}{\Gamma(N_r)\Gamma(N_s)} \left(\frac{\bar{\gamma}}{N_s}\right)^t. \tag{20}$$

where $\mathbb{E}\{\cdot\}$ refers to the expectation operator.

Proof The t th moment of β_{MRC} is

$$\begin{aligned} \mathbb{E}\{\beta_{MRC}^t\} &= \int_0^\infty x^t f_{\beta_{MRC}}(x) dx \\ &= \frac{4}{\Gamma(N_r)\Gamma(N_s)} \left(\frac{1}{N_s}\right)^t \int_0^\infty z^{N_s+N_r-1+2t} K_{N_s-N_r}(2z) dz. \end{aligned} \tag{21}$$

Using [22, Eq. (6.561.16)], we obtain

$$\mathbb{E}\{\beta_{MRC}^t\} = \frac{\Gamma(N_s + t)\Gamma(N_r + t)}{\Gamma(N_r)\Gamma(N_s)} \left(\frac{1}{N_s}\right)^t. \tag{22}$$

Finally, we use $\mathbb{E}\{\gamma_{MRC}^t\} = \bar{\gamma}^t \mathbb{E}\{\beta_{MRC}^t\}$. □

The t th moment of the SNR at the SC output is given by

$$\mathbb{E}\{\gamma_{SC}^t\} = \sum_{k=1}^{N_r} \binom{N_r}{k} (-1)^{k+1} \frac{\Gamma(N_s + t)\Gamma(t + 1)}{\Gamma(N_s)} \left(\frac{\bar{\gamma}}{kN_s}\right)^t. \tag{23}$$

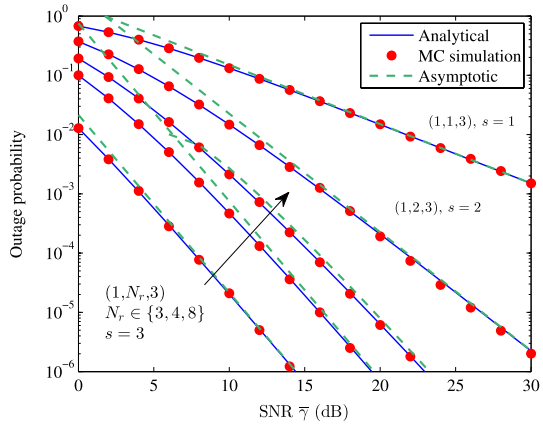
Proof The t th moment of β_{SC} is given by

$$\begin{aligned} \mathbb{E}\{\beta_{SC}^t\} &= \int_0^\infty x^t f_{\beta_{SC}}(x) dx \\ &= \sum_{k=1}^{N_r} \binom{N_r}{k} (-1)^{k+1} \frac{4}{\Gamma(N_s)} \left(\frac{1}{kN_s}\right)^t \int_0^\infty z^{N_s+2t} K_{N_s-1}(2z) dz. \end{aligned} \tag{24}$$

Using [22, Eq. (6.561.16)], we obtain

$$\mathbb{E}\{\beta_{SC}^t\} = \sum_{k=1}^{N_r} \binom{N_r}{k} (-1)^{k+1} \frac{\Gamma(N_s + t)\Gamma(t + 1)}{\Gamma(N_s)} \left(\frac{1}{kN_s}\right)^t. \tag{25}$$

Fig. 3 The P_{out} of different (N_r, N_s) systems with MRC for $\gamma_{th} = 0$ dB



The t th moment of γ_{SC}^t is obtained using $E\{\gamma_{SC}^t\} = \bar{\gamma}^t E\{\beta_{SC}^t\}$. □

4 Performance Analysis

4.1 Outage Probability

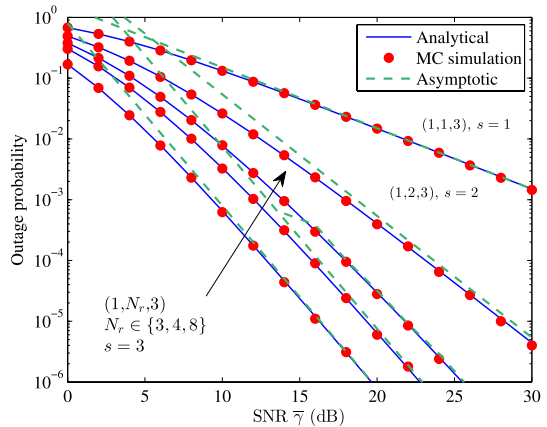
In wireless communications, the outage probability (P_{out}) is an important measurement for the quality-of-service (QoS). It is defined as the probability that the instantaneous received SNR falls below a threshold γ_{th} , i.e.,

$$P_{\text{out}} = \Pr(\gamma \leq \gamma_{th}) = F_{\gamma}(\gamma_{th}). \tag{26}$$

The exact P_{out} of the MRC and SC diversity combining schemes can be evaluated based on (5) and (7), respectively. Asymptotic expressions for the P_{out} for the different scenarios are derived using the CDF approximations in the high SNR regime given in Sect. 3.2.

Figures 3 and 4 show the P_{out} for MRC and SC as a function of the SNR when the threshold γ_{th} is fixed at 0 dB. In these figures, we compare the exact P_{out} , the asymptotic approximations and MC simulated curves for different system configurations. For the rich-scattering i.i.d Rayleigh case ($N_s = \infty$), the P_{out} curves are obtained based on [4, Eq. (7.19) p. 199] for MRC and [4, Eq. (7.8) p. 194] for SC. We can see that the results obtained from analysis match closely those obtained by simulations. It is noted that the slopes of the P_{out} curves are determined by $s = \min(N_s, N_r)$ and that P_{out} diminishes as s increases. Furthermore, we note that as N_s increases, the P_{out} approaches that of rich scattering i.i.d Rayleigh channels. Moreover, we observe that slopes for configurations (4, 2) and (2, 4), which have the same value of s , are identical. However, P_{out} for the (4, 2) system is better than that of (2, 4). The difference is more evident for MRC than for SC. This can be explained by the fact that the array gain increases as N_r increases.

Fig. 4 The P_{out} of different (N_r, N_s) systems with SC for $\gamma_{th} = 0$ dB



4.2 Average Symbol Error Rate

It is well known that the instantaneous SER of many digital modulations can be expressed as [2]

$$P_e(\gamma) = \frac{a}{2} \operatorname{erfc}(\sqrt{b\gamma}), \tag{27}$$

where a and b are specific modulation constants and $\operatorname{erfc}(\cdot)$ is the complementary error function which can be expressed in terms of the Meijer G -function as [25]

$$\operatorname{erfc}(\sqrt{x}) = \frac{1}{\sqrt{\pi}} G_{1,2}^{2,0} \left(x \left| \begin{matrix} 1 \\ 0, \frac{1}{2} \end{matrix} \right. \right). \tag{28}$$

The average SER \bar{P}_e can be derived by averaging the instantaneous SER over the instantaneous SNRs, i.e.,

$$\bar{P}_e = \mathbb{E}\{P_e(\gamma)\} = \int_0^\infty P_e(\gamma) f_\gamma(\gamma) d\gamma. \tag{29}$$

By substituting (6), (27), and (28) into (29) and calculating the resultant integral with the aid of [22, Eq. (7.821.3)], we obtain the closed-form SER expression for the MRC scheme

$$\begin{aligned} \bar{P}_{e,\text{MRC}} &= \mathbb{E}\{P_e(\gamma)\} = \int_0^\infty P_e(\gamma) f_\gamma(\gamma) d\gamma \\ &= \int_0^\infty \frac{aK_{N_s-N_r}(2\sqrt{z})}{\sqrt{\pi}\Gamma(N_r)\Gamma(N_s)} (z)^{\frac{N_s+N_r}{2}-1} G_{1,2}^{2,0} \left(\frac{b\bar{\gamma}}{N_s} z \left| \begin{matrix} 1 \\ 0, \frac{1}{2} \end{matrix} \right. \right) dz \\ &= \frac{aG_{3,2}^{2,2} \left(\frac{b\bar{\gamma}}{N_s} \left| \begin{matrix} 1-N_s, 1-N_r, 1 \\ 0, \frac{1}{2} \end{matrix} \right. \right)}{2\sqrt{\pi}\Gamma(N_r)\Gamma(N_s)}. \end{aligned} \tag{30}$$

By substituting (8), (27), and (28) into (29) and proceeding as in the case of MRC, we can express the SER of the SC scheme as follows

$$\begin{aligned}
 \bar{P}_{e,SC} &= \mathbb{E}\{P_e(\gamma)\} = \int_0^\infty P_e(\gamma)f_\gamma(\gamma)d\gamma \\
 &= \sum_{k=1}^{N_r} \left\{ \frac{a \binom{N_r}{k} (-1)^{k+1}}{\sqrt{\pi}\Gamma(N_s)} \int_0^\infty G_{1,2}^{2,0} \left(\frac{b\bar{\gamma}}{kN_s} z \middle| \begin{matrix} 1, \\ 0, \frac{1}{2} \end{matrix} \right) (z)^{(N_s-1)/2} K_{N_s-1}(2\sqrt{z}) dz \right\} \\
 &= \sum_{k=1}^{N_r} \binom{N_r}{k} (-1)^{k+1} \frac{a G_{3,2}^{2,2} \left(\frac{b\bar{\gamma}}{kN_s} \middle| \begin{matrix} 1-N_s, 0, 1 \\ 0, \frac{1}{2} \end{matrix} \right)}{2\sqrt{\pi}\Gamma(N_s)}.
 \end{aligned} \tag{31}$$

We now investigate the SER performance in the high SNR regime in order to derive the diversity order and the array gain of the two considered schemes. To this end, we consider the approximation of $K_\nu(x)$ for small values of x .

4.2.1 Case I: MRC with $N_r \neq N_s$

By invoking [26, Propo. 1], we express the average SER in the high SNR regime as

$$\bar{P}_{e,MRC}^\infty(\bar{\gamma}) = \frac{aN_s^s \Gamma(|N_s - N_r|) \Gamma(s + \frac{1}{2})}{2\sqrt{\pi}s \Gamma(N_r) \Gamma(N_s)} (b\bar{\gamma})^{-s} + o(\bar{\gamma}^{-s}). \tag{32}$$

Given (32), we conclude that the diversity order for the MRC scheme, when $N_r \neq N_s$ is

$$G_d^{MRC} = \min(N_s, N_r) = s, \tag{33}$$

and the array gain is

$$G_a^{MRC} = b \left(\frac{a2^s N_s^s \Gamma(|N_s - N_r|) \Gamma(s + \frac{1}{2})}{\sqrt{\pi}s \Gamma(N_r) \Gamma(N_s)} \right)^{-1/s}. \tag{34}$$

4.2.2 Case II: MRC with $N_r = N_s$

When $N_r = N_s$, we cannot derive the diversity order using [26, Propo. 1]. In this case, the average SER in the high SNR regime can be obtained by replacing the complementary function by its integral representation and exploiting [22, Eq. (4.352.1)], as suggested in [27], i.e.

$$\begin{aligned}
 \bar{P}_{e,MRC}^\infty(\bar{\gamma}) &= \int_0^\infty P_e(x) f_{\gamma_{MRC}}^\infty(x) dx \\
 &= -\frac{a\sqrt{b}(N_s/\bar{\gamma})^{N_s}}{\sqrt{\pi}[\Gamma(N_s)]^2} \int_1^\infty \int_0^\infty e^{-bt^2 \frac{x}{N_s}} \left(\frac{\bar{\gamma}}{N_s} \right)^{N_s-1/2} x^{N_s-1/2} \ln(x) dx dt \\
 &= \frac{a\Gamma(N_s + \frac{1}{2})}{2N_s\sqrt{\pi}[\Gamma(N_s)]^2} \ln \left(\frac{b\bar{\gamma}}{N_s} \right) \left(\frac{N_s}{b\bar{\gamma}} \right)^{N_s}.
 \end{aligned} \tag{35}$$

The diversity order is given by [28]

$$G_d^{\text{MRC}} = - \lim_{\bar{\gamma} \rightarrow \infty} \frac{\log \bar{P}_{e,\text{MRC}}^\infty}{\log \bar{\gamma}}. \tag{36}$$

Given (35) and using $\lim_{x \rightarrow \infty} \log(cx)/\log(x) = 1$, we conclude that

$$G_d^{\text{MRC}} \approx N_s - 1 = s - 1. \tag{37}$$

Here, we note that given (35), the diversity behavior cannot be described by an integer [29]. In this case, the diversity order falls between $N_s - 1$ and N_s [29, 30].

4.2.3 Case III: SC Scheme with $N_s \leq N_r$

In this case, the asymptotic SER can be expressed as

$$\begin{aligned} \bar{P}_{e,\text{SC}}^\infty(\bar{\gamma}) &= \int_0^\infty P_e(x) f_{\gamma_{\text{SC}}}^\infty(x) dx \\ &= \sum_{k=1}^{N_r} \left\{ \binom{N_r}{k} \frac{(-1)^{k+1+N_s} a \Gamma(N_s + \frac{1}{2})}{2N_s \sqrt{\pi} [\Gamma(N_s)]^2} \ln \left(\frac{b\bar{\gamma}}{kN_s} \right) \left(\frac{kN_s}{b\bar{\gamma}} \right)^{N_s} \right\}. \end{aligned} \tag{38}$$

For this case, the diversity order is

$$G_d^{\text{SC}} \approx N_s - 1 = s - 1. \tag{39}$$

4.2.4 Case IV: SC Scheme with $N_s > N_r$

When $N_s > N_r$, the asymptotic SER of the SC scheme is given by

$$\begin{aligned} \bar{P}_{e,\text{SC}}^\infty(\bar{\gamma}) &= \int_0^\infty P_e(x) f_{\gamma_{\text{SC}}}^\infty(x) dx \\ &= \sum_{k=1}^{N_r} \left\{ \binom{N_r}{k} \frac{a(-1)^{k+N_r} (b\bar{\gamma})^{-N_r} \Gamma(N_r + \frac{1}{2}) (N_s - N_r - 1)! (kN_s)^{N_r}}{2N_r! \Gamma(N_s) \sqrt{\pi}} \right\}. \end{aligned} \tag{40}$$

Given (40), we conclude that the diversity order is

$$G_d^{\text{SC}} = N_r = s. \tag{41}$$

To validate the derived SER expressions, MC simulations have been carried out for different Rayleigh product (N_r, N_s) channels. The results are obtained for quadrature phase-shift keying (QPSK) modulation ($a = 2, b = 0.5$). The average SER of MRC and SC schemes are, respectively, shown in Figs. 5 and 6, where exact SER, asymptotic approximations and MC results are compared. For further comparison, the average SER of rich-scattering i.i.d Rayleigh channels is also presented. For this case, the SER curves for MRC and SC are obtained from [31, Eq. (12)] and [31, Eq. (23)], respectively. For all scenarios, there is excellent agreement between the exact and asymptotic analytical SER expressions and MC results. It is noted that slopes of SER curves are proportional to the diversity order and as N_s increases, the average SER approaches that of rich scattering i.i.d Rayleigh channels. Moreover, for $N_s \geq 4$, the slopes of SER curves are identical to that of

Fig. 5 SER of QPSK versus SNR $\bar{\gamma}$ in $(4, N_s)$ channels with MRC

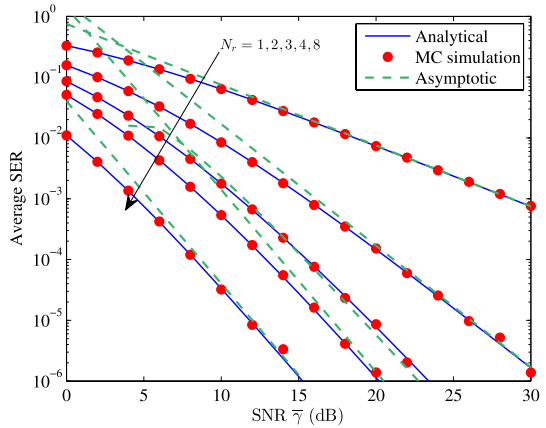
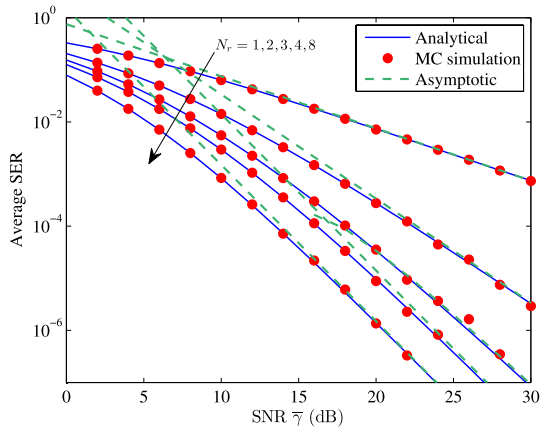


Fig. 6 SER of QPSK versus SNR $\bar{\gamma}$ in $(4, N_s)$ channels with SC



the rich-scattering case. In fact, for $N_s \geq 4$, we have $s = N_r = 4$ which corresponds to the diversity order of MRC and SC in i.i.d Rayleigh channels.

4.3 Ergodic Capacity

Here, we derive closed-form expressions for the ergodic capacity defined as the expectation of the instantaneous mutual information, i.e.

$$C = \mathbb{E}\{\log_2(1 + \gamma)\} = \int_0^\infty \log_2(1 + \gamma)f_\gamma(\gamma)d\gamma. \tag{42}$$

For the MRC scheme, the ergodic capacity is given by

$$C = \int_0^\infty \log_2(1 + \gamma) \frac{2\gamma^{\frac{N_s+N_r}{2}-1}}{\Gamma(N_r)\Gamma(N_s)} \left(\frac{N_s}{\bar{\gamma}}\right)^{\frac{N_s+N_r}{2}} K_{N_s-N_r}\left(2\sqrt{\gamma N_s/\bar{\gamma}}\right) d\gamma. \tag{43}$$

Using [32, Eq. (8.4.6.5)], [22, Eq. (9.31.2)] and, [22, Eq. (7.821.3)], we can express the ergodic capacity as

$$C = \frac{1}{\Gamma(N_r)\Gamma(N_s)\ln 2} G_{2,4}^{4,1} \left(\frac{N_s}{\bar{\gamma}} \mid 0, 1 \mid N_s, N_r, 0, 0 \right). \tag{44}$$

For the SC scheme, the ergodic capacity is given by

$$\begin{aligned} C &= \int_0^\infty \log_2(1 + \gamma) f_{\gamma_{SC}}(\gamma) d\gamma \\ &= \sum_{k=1}^{N_r} \binom{N_r}{k} (-1)^{k+1} \frac{2}{\Gamma(N_s)} \left(\frac{kN_s}{\bar{\gamma}} \right)^{\frac{N_s+1}{2}} \\ &\quad \times \int_0^\infty \log_2(1 + \gamma) \gamma^{\frac{N_s-1}{2}} K_{N_s-1} \left(2\sqrt{k\gamma N_s/\bar{\gamma}} \right) d\gamma. \end{aligned} \tag{45}$$

Using [32, Eq. (8.4.6.5)], [22, Eq. (9.31.2)] and [22, Eq. (7.821.3)], we can express the ergodic capacity as

$$C = \sum_{k=1}^{N_r} \left\{ \binom{N_r}{k} (-1)^{k+1} \frac{1}{\Gamma(N_s)\ln 2} G_{2,4}^{4,1} \left(\frac{kN_s}{\bar{\gamma}} \mid 0, 1 \mid N_s, 1, 0, 0 \right) \right\}. \tag{46}$$

4.3.1 High SNR Capacity

For high SNR values, the capacity can be expressed as [16, 33]

$$C(\bar{\gamma}) = S_\infty \left(\frac{\bar{\gamma}|_{\text{dB}}}{3 \text{ dB}} - \mathcal{L}_\infty \right) + o(1), \tag{47}$$

where $3 \text{ dB} = 10 \log_{10}(2)$ and the S_∞ and \mathcal{L}_∞ are defined as

$$S_\infty = \lim_{\bar{\gamma} \rightarrow \infty} \frac{C(\bar{\gamma})}{\log_2(\bar{\gamma})}, \tag{48}$$

$$\mathcal{L}_\infty = \lim_{\bar{\gamma} \rightarrow \infty} \left(\log_2(\bar{\gamma}) - \frac{C(\bar{\gamma})}{S_\infty} \right). \tag{49}$$

Given (53), it was shown in [33] that $S_\infty = 1 \text{ bit/s/Hz}$, regardless of N_r and N_s . The high SNR power offset \mathcal{L}_∞ is derived by substituting (53) in (49) as [16]

$$\mathcal{L}_\infty = -\log_2(e) \frac{d}{dt} \left(\mathbb{E}[\beta_1^t] \right) \Big|_{t=0}. \tag{50}$$

For the MRC scheme, by substituting (22) in (50) and calculating the resultant derivative with the aid of the identity $d\Gamma(z)/dz = \psi(z)\Gamma(z)$, we express $\mathcal{L}_\infty^{\text{MRC}}$ as

$$\mathcal{L}_\infty^{\text{MRC}} = -\log_2(e) [\psi(N_r) + \psi(N_s) - \ln N_s]. \tag{51}$$

For the SC technique, $\mathcal{L}_\infty^{\text{SC}}$ is given by

$$\mathcal{L}_\infty^{\text{SC}} = \log_2(e) \sum_{k=1}^{N_r} \binom{N_r}{k} (-1)^k [\psi(N_s) + \psi(1) - \ln(kN_s)]. \tag{52}$$

Fig. 7 Ergodic capacity of $(N_r, 3)$ channels with MRC

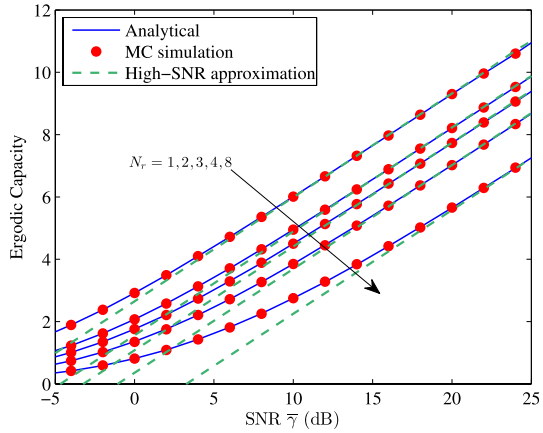
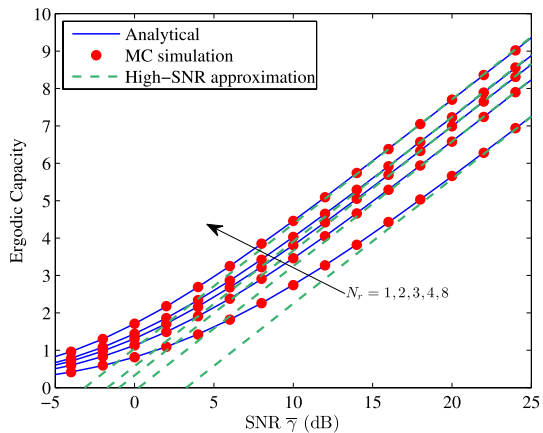


Fig. 8 Ergodic capacity of $(N_r, 3)$ channels with SC



Exact ergodic capacity expressions and analytical high SNR capacity approximations are compared with MC simulated capacity results in Figs. 7 and 8. We observe perfect agreement between analytical curves and simulation results. As expected, for all cases, the high SNR slopes of capacity curves are unity, since $S_\infty = 1$ bit/s/Hz. Thus, increasing N_r serves only to improve the high SNR power offset \mathcal{L}_∞ .

4.3.2 Low SNR Capacity

Authors in [34–36] have shown that taking the first-order expansion of the ergodic capacity as $\bar{\gamma} \rightarrow 0$ to investigate the channel impact in the low SNR regime is not relevant [37]. In this SNR regime, to characterize the tradeoff between channel capacity, bandwidth and power, it is appropriate to consider the normalized transmit energy per information bit E_b/N_0 rather the SNR [34–37]. As discussed in [36], for low values of E_b/N_0 , the capacity is approximated by [34–37]

$$C\left(\frac{E_b}{N_0}\right) \approx S_0 \log_2 \left(\frac{\frac{E_b}{N_0}}{\frac{E_b}{N_{0 \min}}} \right), \tag{53}$$

where $(E_b/N_{0 \min})$ is the minimum E_b/N_0 required for reliable communication and S_0 is the spectral efficiency slope in bits/s/Hz. From [36], the two parameters are given by

$$\frac{E_b}{N_{0 \min}} = \frac{\ln 2}{\mathbb{E}\{\beta_i\}}, \tag{54}$$

and

$$S_0 = \frac{2(\mathbb{E}\{\beta_i\})^2}{\mathbb{E}\{\beta_i^2\}}. \tag{55}$$

Using (22), we obtain the r th moment of β_{MRC} which yields

$$\frac{E_b}{N_{0 \min}}^{\text{MRC}} = \frac{\ln 2}{N_r}, \tag{56}$$

and

$$S_0^{\text{MRC}} = \frac{2N_r N_s}{(N_r + 1)(N_s + 1)}. \tag{57}$$

From (56), we can observe that $\frac{E_b}{N_{0 \min}}^{\text{MRC}}$ is inversely proportional to the number of available branches N_r and is independent of N_s . Furthermore, the minimum required received bit energy above noise level, which is a fundamental feature for channels with additive Gaussian noise [34–37], is equal to

$$\frac{E_b}{N_{0 \min}}^{\text{MRC},r} = N_r \frac{E_b}{N_{0 \min}}^{\text{MRC}} = -1.59 \text{ dB} \tag{58}$$

It is noted that N_r and N_s do not affect this metric.

For the SC scheme, the identity (25) leads to

$$\frac{E_b}{N_{0 \min}}^{\text{SC}} = \frac{\ln 2}{\sum_{k=1}^{N_r} \binom{N_r}{k} (-1)^{k+1} k^{-1}}, \tag{59}$$

and

$$S_0^{\text{SC}} = \frac{N_s}{N_s + 1} \frac{\left(\sum_{k=1}^{N_r} \binom{N_r}{k} (-1)^{k+1} k^{-1} \right)^2}{\sum_{k=1}^{N_r} \binom{N_r}{k} (-1)^{k+1} k^{-2}}. \tag{60}$$

Here, we can see that $\frac{E_b}{N_{0 \min}}^{\text{SC}}$ depends only on N_r , and unlike the MRC case, $\frac{E_b}{N_{0 \min}}^{\text{SC},r}$ also depends on N_r .

Fig. 9 Low-SNR ergodic capacity for $(4, N_s)$ channels with MRC

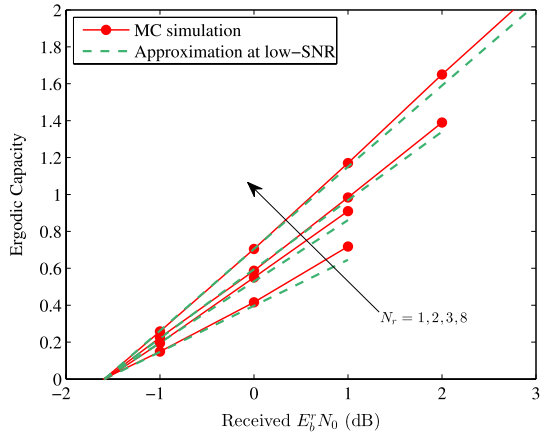
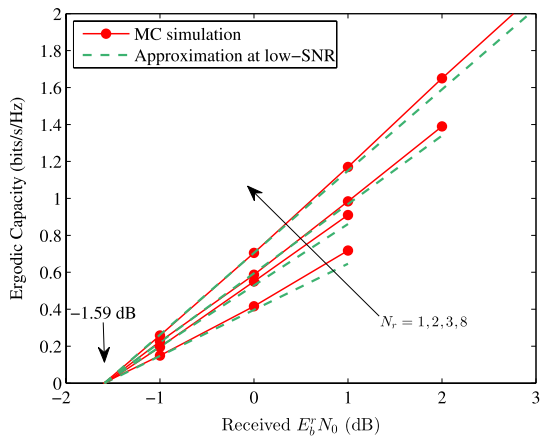
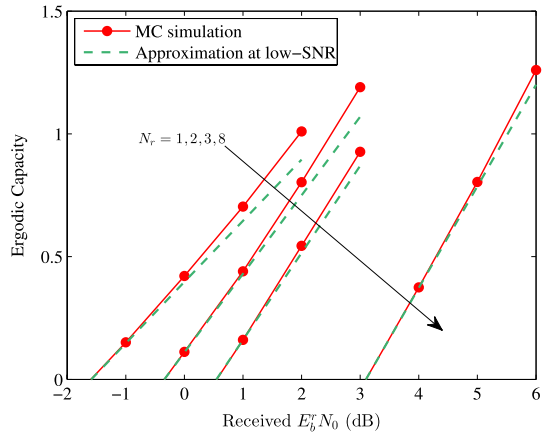


Fig. 10 Low-SNR ergodic capacity for $(N_r, 3)$ channels with MRC



In Figs. 9, 10 and 11, we compare the low SNR capacity approximations with MC simulated ergodic capacity. The ergodic capacity and its low SNR approximation are depicted versus $\frac{E_b}{N_0} r$ for different channel configurations. As we can see, the low SNR approximations are quite tight for all considered cases. Figure 9 illustrates the impact of N_s on the low SNR capacity and confirms the intuitive result that the capacity improves as N_s increases to converge to that of i.i.d Rayleigh channels. In Fig. 10, the low SNR approximations are presented for different values on N_r . As expected, the low SNR slope increases with N_r , whereas $\frac{E_b}{N_0} \text{MRC}, r = -1.59$ dB regardless of N_r and N_s . For $N_s = 20$ and $N_s = \infty$, the low SNR slope is about 1.56 bits/s/Hz per 3 dB. However, for $N_s = 1$ (keyhole channel), the slope is reduced to 1.02 dB. Hence, the discrepancy between the two extreme cases is about 35%. In Fig. 11, we consider the SC combiner and investigate the impact of N_r and N_s on the the low SNR capacity. It is noted that the minimum received bit energy above noise level required for reliable communication depends on N_r .

Fig. 11 Low-SNR ergodic capacity for $(2, N_s)$ and $(4, N_s)$ channels with SC



5 Conclusion

An analytical performance assessment of the MRC and SC diversity schemes over Rayleigh product channels was presented. Exact closed-form expressions and asymptotic expansions of the CDF and PDF of the SNR at each combiner output were derived. Exact expressions were the starting point to derive closed-form formulas for the OP, the average SER and the channel capacity. Based on the asymptotic approximations of the PDFs, we evaluated the asymptotic SER which accurately reveals the diversity order and the array gain. We have shown that the diversity gain depends on the minimum of the numbers of scatterers and available branches. Furthermore, when the number of scatterers becomes sufficiently large, the system performance approaches that of i.i.d Rayleigh channels. We have also characterized the channel capacity in high and low SNR regimes by deriving closed-form expressions for key parameters such as high SNR power offset \mathcal{L}_∞ , high SNR slope in S_∞ , the minimum required transmit energy per information bit $\frac{E_b}{N_0 \min}$ and the spectral efficiency slope S_0 .

6 Proof of Proposition 1

Let $\mathbf{g}\mathbf{g}^H = \mathbf{U}\mathbf{S}\mathbf{V}^H$ be the singular value decomposition of $\mathbf{g}\mathbf{g}^H$, where $\mathbf{S} \in \mathbb{C}^{N_s \times N_s}$ is a diagonal matrix, and \mathbf{U} and \mathbf{V} are two $N_s \times N_s$ unitary matrices. We can express $\|\mathbf{H}_1 \mathbf{g}\|_F^2$ as

$$\|\mathbf{H}_1 \mathbf{g}\|_F^2 = \text{tr}(\mathbf{H}_1 \mathbf{U} \mathbf{S} \mathbf{V}^H \mathbf{H}_1^H). \tag{61}$$

Given that \mathbf{U} and \mathbf{V} are unitary matrices, conditioned on \mathbf{g} , we have

$$\mathbf{H}_1 \mathbf{U} \mathbf{S} \mathbf{V}^H \mathbf{H}_1^H | \mathbf{g} \sim \mathbf{H}_1 \mathbf{S} \mathbf{H}_1^H | \mathbf{g}, \tag{62}$$

where “ \sim ” denotes equivalent distribution. Since $\mathbf{H}_1 \mathbf{g}$ is a vector, $\mathbf{H}_1 \mathbf{g}\mathbf{g}^H \mathbf{H}_1^H$ is a rank one Hermitian matrix with only one non-zero eigenvalue, which corresponds to $S_{11} = \|\mathbf{g}\|_F^2$. Hence, it can easily be observed that, conditioned on \mathbf{g} , we have

$$\|\mathbf{h}\|_F^2 \sim \text{tr}(\mathbf{H}_1 \mathbf{S} \mathbf{H}_1^H) \sim \|\mathbf{g}\|_F^2 \|\mathbf{h}_{1,1}\|_F^2. \tag{63}$$

Since the entries of \mathbf{H}_1 are zero-mean unit-variance complex-Gaussian random variables, $\|\mathbf{h}_{1,1}\|_F^2$ is a Chi-squared variate with $2N_r$ degrees of freedom. Thus, using a change of variable, we can show that the conditioned CDF and PDF of the received SNR are given by

$$F_{\beta_{\text{MRC}}}(x|\mathbf{g}) = 1 - e^{-\frac{xN_s}{\|\mathbf{g}\|_F^2}} \sum_{l=0}^{N_r-1} \frac{1}{l!} \left(\frac{xN_s}{\|\mathbf{g}\|_F^2}\right)^l, \tag{64}$$

$$f_{\gamma_{\text{MRC}}}(x|\mathbf{g}) = \frac{N_s^{N_r} x^{N_r-1} e^{-xN_s/(\|\mathbf{g}\|_F^2)}}{\Gamma(N_r)(\|\mathbf{g}\|_F^2)^{N_r}}.$$

The PDF of the Chi-squared distributed random variable $Z = \|\mathbf{g}\|_F^2$ is

$$f_Z(z) = \frac{1}{\Gamma(N_s)} z^{N_s-1} e^{-z}. \tag{65}$$

The unconditional CDF of β_{MRC} can be obtained as follows

$$F_{\beta_{\text{MRC}}}(x) = \int_0^{+\infty} F_{\beta_{\text{MRC}}}(x|\mathbf{g}) f_Z(z) dz$$

$$= 1 - \sum_{l=0}^{N_r-1} \left\{ \frac{(xN_s)^l}{\Gamma(N_s)l!} \int_0^{+\infty} \exp\left(-z - \frac{xN_s}{z}\right) z^{N_s-l-1} dz \right\}. \tag{66}$$

Using [22, Eq. (3.471.9)], we obtain the closed-form CDF expression

$$F_{\beta_{\text{MRC}}}(x) = 1 - \sum_{l=0}^{N_r-1} \frac{2(xN_s)^{\frac{N_s+l}{2}}}{\Gamma(N_s)l!} K_{N_s-l}\left(2\sqrt{xN_s}\right). \tag{67}$$

The unconditional PDF of $\gamma_{\beta_{\text{MRC}}}$ can be obtained as

$$f_{\beta_{\text{MRC}}}(x) = \int_0^{+\infty} f_{\beta_{\text{MRC}}}(x|\mathbf{g}) f_Z(z) dz$$

$$= \int_0^{+\infty} \frac{N_s^{N_r} x^{N_r-1}}{\Gamma(N_r)\Gamma(N_s)} z^{N_s-N_r-1} \exp\left(-z - \frac{xN_s}{z}\right) dz. \tag{68}$$

Using [22, Eq. (3.471.9)], we obtain the closed-form PDF expression

$$f_{\beta_{\text{MRC}}}(x) = \frac{2N_s^{\frac{N_s+N_r}{2}} x^{\frac{N_s+N_r-2}{2}}}{\Gamma(N_r)\Gamma(N_s)} K_{N_s-N_r}\left(2\sqrt{xN_s}\right). \tag{69}$$

Using $F_{\gamma_{\text{MRC}}}(x) = F_{\beta_{\text{MRC}}}(x/\bar{\gamma})$ and $f_{\gamma_{\text{MRC}}}(x) = F_{\beta_{\text{MRC}}}(x/\bar{\gamma})/\bar{\gamma}$, we obtain the identities of Proposition 1.

7 Proof of Proposition 2

Let us first consider the conditioned CDF and PDF of the received SNR at any antenna i given \mathbf{g} . By substituting $N_r = 1$ into (64), we obtain the CDF and the PDF of $\beta^i = |h_i|^2$, i.e.

$$\begin{aligned} F_{\beta^i}(x|\mathbf{g}) &= 1 - e^{-\frac{xN_s}{\|\mathbf{g}\|_F^2}}, \\ f_{\beta^i}(x|\mathbf{g}) &= \frac{N_s e^{-xN_s/\|\mathbf{g}\|_F^2}}{\|\mathbf{g}\|_F^2}. \end{aligned} \quad (70)$$

Given \mathbf{g} , the conditioned β^i are independent and identically distributed since the rows of \mathbf{H}_1 are i.i.d.². Hence, thanks to order statistics, the conditioned CDF and PDF of β_{SC} can be expressed as [25]

$$\begin{aligned} F_{\beta_{\text{SC}}}(x|\mathbf{g}) &= [F_{\beta^i}(x|\mathbf{g})]^{N_r}, \\ f_{\beta_{\text{SC}}}(x|\mathbf{g}) &= N_r f_{\beta^i}(x|\mathbf{g}) [F_{\beta^i}(x|\mathbf{g})]^{N_r-1}. \end{aligned} \quad (71)$$

The unconditional CDF of β_{SC} is given by

$$\begin{aligned} F_{\beta_{\text{SC}}}(x) &= \int_0^{+\infty} F_{\beta_{\text{SC}}}(x|\mathbf{g}) f_Z(z) dz \\ &= 1 + \sum_{k=1}^{N_r} \binom{N_r}{k} \frac{2(-1)^k (kxN_s)^{\frac{N_s}{2}}}{\Gamma(N_s)} K_{N_s} \left(2\sqrt{kxN_s} \right). \end{aligned} \quad (72)$$

To compute the PDF, we take the derivative of the CDF using [16, Eq. (99)]

$$\frac{d}{dx} ((\alpha x)^{\nu/2} K_{\nu}(2\sqrt{\alpha x}) = -\alpha (\alpha x)^{(\nu-1)/2} K_{\nu-1}(2\sqrt{\alpha x}), \quad (73)$$

The unconditional PDF of β_{SC} is given by

$$f_{\beta_{\text{SC}}}(x) = \sum_{k=1}^{N_r} \binom{N_r}{k} (-1)^{k+1} \frac{2kN_s}{\Gamma(N_s)} (kxN_s)^{\frac{N_s-1}{2}} K_{N_s-1} \left(2\sqrt{kxN_s} \right). \quad (74)$$

The CDF and PDF of γ_{SC} are obtained in a straightforward manner from (72) and (74).

References

1. Brennan, D. (1959). Linear diversity combining techniques. *Proceedings of the IRE*, 47(6), 1075.
2. Proakis, J., & Salehi, M. (2007). *Digital communications* (5th ed.). New York City: McGraw-Hill Higher Education.
3. Eng, T., Kong, N., & Milstein, L. B. (1996). Comparison of diversity combining techniques for Rayleigh-fading channels. *IEEE Transactions on Communication*, 44(9), 1117.
4. Goldsmith, A. (2005). *Wireless communications*. Cambridge: Cambridge University Press.

² We note that the unconditional β^i are dependent. Hence, the order statistics analysis of the unconditional SNRs is complicate.

5. Simon, M. K., & Alouini, M. S. (1998). A unified approach to the performance analysis of digital communication over generalized fading channels. *Proceedings of the IEEE*, 86(9), 1860.
6. Simon, M. K., & Alouini, M. S. (2005). *Digital communication over fading channels* (1st ed.). Hoboken: Wiley-Interscience.
7. Pierce, J., & Stein, S. (1960). Multiple diversity with nonindependent fading. *Proceedings of the IRE*, 48(1), 89.
8. Aalo, V. (1995). Performance of maximal-ratio diversity systems in a correlated Nakagami-fading environment. *IEEE Transactions on Communications*, 43(8), 2360.
9. Luo, J., Zeidler, J., & McLaughlin, S. (2001). Performance analysis of compact antenna arrays with MRC in correlated Nakagami fading channels. *IEEE Transactions on Vehicular Technology*, 50(1), 267.
10. Win, M. Z., Chrisikos, G., & Winters, J. H. (2000). MRC performance for M -ary modulation in arbitrarily correlated Nakagami fading channels. *IEEE Communications Letters*, 4(10), 301.
11. Dietze, K., Dietrich, C. B., & Stutzman, W. L., (2002). Analysis of a two-branch maximal ratio and selection diversity system with unequal SNRs and correlated inputs for a Rayleigh fading channel. *IEEE Transactions on Wireless Communications*, 1(2), 274.
12. Zhang, Q., & Lu, H. (2002). A general analytical approach to multi-branch selection combining over various spatially correlated fading channels. *IEEE Transactions on Communications*, 50(7), 1066.
13. Gesbert, D., Bolcskei, H., Gore, D. A., & Paulraj, A. J. (2002). Outdoor MIMO wireless channels: models and performance prediction. *IEEE Transactions on Communications*, 50(12), 1926.
14. Almers, P., Tufvesson, F., & Molisch, A. F. (2006). Keyhole effect in MIMO wireless channels: Measurements and theory. *IEEE Transactions on Wireless Communications*, 5(12), 3596.
15. Zhong, C., Ratnarajah, T., Zhang, Z., Wong, K. K., & Sellathurai, M. (2014). Performance of rayleigh-product MIMO channels with linear receivers. *IEEE Transactions on Wireless Communications*, 13(4), 2270.
16. Jin, S., McKay, M. R., Wong, K. K., & Gao, X. (2008). Transmit beamforming in Rayleigh product MIMO channels: Capacity and performance analysis. *IEEE Transactions on Signal Processing*, 56(10), 5204.
17. Zhong, C., Jin, S., & Wong, K. K. (2009). MIMO rayleigh-product channels with co-channel interference. *IEEE Transactions on Communications*, 57(6), 1824.
18. Wu, Y., Jin, S., Gao, X., Xiao, C., & McKay, M. R. (2012). MIMO multichannel beamforming in Rayleigh-product channels with arbitrary-power co-channel interference and noise. *IEEE Transactions on Wireless Communications*, 11(10), 3677.
19. Wongtrairat, W., & Supnithi, P. (2009). Performance of digital modulation in double Nakagami- m fading channels with MRC diversity. *IEICE Transactions on Communications*, E92.B(2), 559.
20. Talha, B., Patzold, M., & Primak, S. (2010). In *2010 IEEE international conference on communications workshops (ICC)*
21. Bithas, P. S., Kanatas, A. G., da Costa, D. B., Upadhyay, P. K., & Dias, U. S. (2018). On the double-generalized gamma statistics and their application to the performance analysis of V2V communications. *IEEE Transactions on Communications*, 66(1), 448.
22. Gradshteyn, I., & Ryzhik, I. (2007). *Table of integrals, series, and products* (7th ed.). Cambridge: Academic Press.
23. Zhang, Y., & Tepedelenioglu, C. (2012). Applications of Tauberian theorem for high-SNR analysis of performance over fading channels. *IEEE Transactions on Wireless Communications*, 11(1), 296.
24. Bingham, N. H., Goldie, C. M., & Teugels, J. L. (1989). *Regular variation* (Vol. 27). Cambridge: Cambridge University Press.
25. Chen, Z., Yuan, J., & Vucetic, B. (2005). Analysis of transmit antenna selection/maximal-ratio combining in Rayleigh fading channels. *IEEE Transactions on Vehicular Technology*, 54(4), 1312.
26. Wang, Z., & Giannakis, G. (2003). A simple and general parameterization quantifying performance in fading channels. *IEEE Transactions on Communications*, 51(8), 1389.
27. Muller, A., & Speidel, J. (2006). In *First international conference on communications and networking in China, 2006. ChinaCom'06*
28. Zheng, L., & Tse, D. N. C. (2003). Diversity and multiplexing: A fundamental tradeoff in multiple-antenna channels. *IEEE Transactions on Information Theory*, 49(5), 1073.
29. Sanayei, S., & Nosratinia, A. (2007). Antenna selection in keyhole channels. *IEEE Transactions on Communications*, 55(3), 404.
30. Sanayei, S., Hedayat, A., & Nosratinia, A. (2007). Space-time codes in keyhole channels: Analysis and design. *IEEE Transactions on Wireless Communications*, 6(6), 2006.
31. Lu, J., Tjhung, T., & Chai, C. (1998). Error probability performance of L -branch diversity reception of MQAM in rayleigh fading. *IEEE Transactions on Communications*, 46(2), 179.

32. Prudnikov, A. P., Brychkov, Y. A., & Marichev, O. I. (1990). *Integrals and series, volumn 3: More special functions*. London: Gordon and Breach.
33. Lozano, A., Tulino, A., & Verdu, S. (2005). High-SNR power offset in multiantenna communication. *IEEE Transactions on Information Theory*, 51(12), 4134.
34. Verdu, S. (2002). Spectral efficiency in the wideband regime. *IEEE Transactions on Information Theory*, 48(6), 1319.
35. Lozano, A., Tulino, A., & Verdu, S. (2003). Multiple-antenna capacity in the low-power regime. *IEEE Transactions on Information Theory*, 49(10), 2527.
36. Shamai, S., & Verdu, S. (2001). The impact of frequency-flat fading on the spectral efficiency of CDMA. *IEEE Transactions on Information Theory*, 47(4), 1302.
37. Shin, H., & Win, M. Z. (2008). MIMO diversity in the presence of double scattering. *IEEE Transactions on Information Theory*, 54(7), 2976.

Publisher's Note Springer Nature remains neutral with regard to jurisdictional claims in published maps and institutional affiliations.



Mohamed Lassaad Ammari received the engineering degree from the University of Carthage, Tunis, Tunisia, in 1995 and the M.Sc. and the Ph.D. Degrees from Université Laval, Quebec City, QC, Canada, in 2000 and 2003, respectively. From 2003 to 2005, he was a Research Associate with the Laboratory of Communications and Integrated Microelectronics, École de Technologie Supérieure, Montreal, QC. He is currently a Professor with the National Engineering School of Sousse, Sousse, Tunisia. He is also an active team member with the Innovation of Communicant and Cooperative Mobiles Laboratory, Higher School of Communications of Tunis, University of Carthage. His research interests include channel equalization, multiple-input-multiple-output orthogonal frequency-division multiplexing systems, turbo detection, space-time coding, and adaptive modulation.



Sébastien Roy received the B.Sc.A. and M.Sc. Degrees in Electrical Engineering from Université Laval, Québec, QC, Canada, in 1991 and 1993, respectively, and the Ph.D. Degree from Carleton University, Ottawa, ON, Canada, in 2000. From 2000 to 2002, he was a National Sciences and Engineering Research Council of Canada Post-doctoral Fellow, Université Laval. In 2007, 2009, and 2011, he was an Invited Professor with the École Nationale Supérieure de Sciences Appliquées et de Technologie, Lannion, France. In 2015, he was an Invited Professor with the Institut National de Sciences Appliquées, Rennes, France. From 2002 to 2012, he was successively promoted to an Assistant, an Associate (from 2005), and a Full Professor (from 2010) with Université Laval. In 2012, he joined the Electrical and Computer Engineering Department, The Université de Sherbrooke, Sherbrooke, QC, Canada, where he is currently a Full Professor and the Department Chair, and where he is currently involved in system-oriented and implementation aspects of signal processing for advanced wireless communications. He is also a co-founder and a co-leader of the Center of Excellence in

Integrated Intelligent Systems, The Université de Sherbrooke. He has been active in industrial consulting and was involved in the organization of several international conferences. He received the Award for the Post-graduate Research Excellence from the Canadian Institute for Telecommunications Research in 2000. He was also a recipient of multiple teaching awards and the Industrial Collaboration Award from the provincial strategic network in advanced systems and technologies for communications in 2007.